

## PAPER



Cite this: *J. Mater. Chem. A*, 2015, 3, 2895

# Superwetting polymer-decorated SWCNT composite ultrathin films for ultrafast separation of oil-in-water nanoemulsions†

Shou Jian Gao,<sup>ab</sup> Yu Zhang Zhu,<sup>a</sup> Feng Zhang<sup>a</sup> and Jian Jin<sup>\*a</sup>

Functional membranes with a superwetting surface property have been extensively explored to achieve oil–water separation. Here, single-walled carbon nanotube/polydopamine/polyethyleneimine (SWCNT/PD/PEI) composite ultrathin films which have superhydrophilic and underwater superoleophobic properties were successfully prepared and used for the ultrafast separation of surfactant-stabilized oil-in-water nanoemulsions containing oil droplets of tens of nanometers. A SWCNT/PD/PEI composite film with an effective pore size of  $\sim 10$  nm and a thickness of  $\sim 160$  nm can effectively separate oil-in-water nanoemulsions in an ultrafast manner with fluxes up to  $\sim 6000$  L m<sup>−2</sup> h<sup>−1</sup> bar<sup>−1</sup>, which is 10-fold higher than traditional ultrafiltration membranes with a similar rejection property. Meanwhile, this film exhibits excellent pH-stability and antifouling property. This work points a direction for designing and fabricating ultrathin and superwetting films for the effective separation of oil-in-water nanoemulsions or nano-sized oils which are hard to separate by traditional methods. The SWCNT/PD/PEI ultrathin film holds promising potential for purifying emulsified wastewater from industries and daily life and for drinking water treatment.

Received 21st October 2014  
Accepted 15th December 2014

DOI: 10.1039/c4ta05624h

www.rsc.org/MaterialsA

## Introduction

Oil related activities in modern industrialization promote economic growth and social development, and simultaneously give rise to severe environmental pollution.<sup>1,2</sup> Emulsified oil-in-water is one of the most important and intractable pollution sources affecting and harming the environment and people's health in a wide range of ways.<sup>3,4</sup> What is worse, emulsified oils from industries and daily life will further aggravate the shortage crisis of drinkable freshwater.<sup>5,6</sup> Removing emulsified oil from water has become a worldwide subject which is tough and challenging.<sup>1,7</sup> Traditional techniques for oil–water separation such as skimming technologies, flotation technologies, settling tanks, and coagulation *etc.* are process-complex, energy-intensive and not effective for emulsified oil–water mixtures.<sup>8,9</sup>

Polymer-based or ceramic-based filtration membranes have been acknowledged as some of the advanced technologies for removing emulsified oils from water with acceptable discharge standards and a relatively simple process which is better than other techniques.<sup>10–14</sup> However, traditional filtration membranes suffer from a very low permeation flux due to their relatively thick separation layer and quick decline of permeation due to serious oil fouling.<sup>15–18</sup> New advanced separation membranes as alternatives to the traditional membranes for the ultrafast separation of emulsified oil from water are highly desired.

Recently, a series of progresses on oil–water separation have been made by designing and fabricating superwetting materials with either superhydrophobic–superoleophilic or superhydrophilic–superoleophobic surfaces in combination with surface chemistry and surface roughness.<sup>19–30</sup> Various filtration membranes with superwetting surfaces have been explored and used to separate emulsified oils from water.<sup>31–39</sup> However, most of these are mesh-based membranes with an effective pore size at the micrometer scale, and thus are only applicable for the separation of emulsions containing micrometer-scale oil droplets, but incapable of treating nanoemulsions containing nanometer-scale oil droplets, especially for nanoemulsions with oil droplets of tens of nanometers in size.<sup>22,24,27,35</sup> In fact, nanoemulsions or nano-sized oils extensively exist in real wastewater generated from diverse industrial processes, such as the petrochemical, food, steel, medicine and pesticide industries.<sup>40–43</sup> Nanoemulsions or nano-sized oils could cause serious and long-term harm to the environment and people's health

<sup>a</sup>Nano-Bionics Division and i-Lab, Suzhou Institute of Nano-Tech and Nano-Bionics, Chinese Academy of Sciences, Suzhou, 215123, China. E-mail: jjin2009@sinano.ac.cn

<sup>b</sup>Nano Science and Technology Institute, University of Science and Technology of China, Suzhou, 215123, China

† Electronic supplementary information (ESI) available: SWCNT/PD composite films fabricated with different usage of SWCNT/PD; SEM image of Au nanoparticles rejected by the SWCNT/PD composite film; underwater oil adhesion force on the SWCNT/PD/PEI composite film; free-standing SWCNT/PD/PEI composite film showing good flexibility and strength; digital photos and oil droplet size distribution of the oil-in-water nanoemulsions before and after separation; summary of the SWCNT/PD/PEI composite film and its separation performance for oil-in-water nanoemulsions; comparison between the SWCNT/PD/PEI film and other oil–water separation membranes for oil-in-water emulsions with nano-sized oils. See DOI: 10.1039/c4ta05624h

because they are thermodynamically and kinetically stable and hard to treat by traditional separation membranes.<sup>40,44</sup> The effective separation of nanoemulsions or nano-sized oils from water is important and has become a new challenge in the field of wastewater treatment.

A desirable membrane for oil-in-water nanoemulsion separation is expected to have a high permeation flux as well as a high separation efficiency which requires its effective pore size to be small enough to remove the smallest oil droplets. According to the classical Hagen–Poiseuille equation:

$$J = \varepsilon \pi r_p^2 \Delta p / 8 \mu L \quad (1)$$

where the filtration rate  $J$  is directly proportional to the square of the effective pore size  $r_p$  and inversely proportional to the thickness of the membrane  $L$ .<sup>45</sup> It indicates that an ideal membrane should have a selective layer as thin as possible and doesn't sacrifice its effective pore size.<sup>46</sup> However, it is hard to achieve in the conventional systems of polymeric, ceramic and mesh-based membranes. It is highly desirable to design and develop new types of membranes with advanced structures to achieve the above goals to separate oil-in-water nanoemulsions fast and efficiently. In this work, we report the fabrication of superhydrophilic and underwater superoleophobic single-walled carbon nanotube/polydopamine/polyethyleneimine (SWCNT/PD/PEI) composite films with a tunable effective pore size and ultrathin thickness at the nanometer scale *via* a simple and facile approach. A 158 nm-thick SWCNT/PD/PEI composite film with a pore size of  $\sim 10$  nm can separate oil-in-water nanoemulsions ultrafast with a very high permeation flux of up to  $6000 \text{ L m}^{-2} \text{ h}^{-1} \text{ bar}^{-1}$ , which is 10 times higher than that of traditional ultrafiltration membranes with a similar rejection property, and with a high separation efficiency. Meanwhile, the film exhibits excellent pH-stability and anti-fouling properties, superior to most of the polymer or ceramic-based membranes. These advantages make it useful for treating emulsified oil–water mixtures in extreme pH conditions. The SWCNT/PD/PEI composite ultrathin films have great potential to be used as advanced separation membranes for treating and recycling emulsified wastewater and drinking water composed of nano-sized oils.

## Experimental section

### Materials

The SWCNTs (OD:  $< 2$  nm, length:  $5\text{--}30 \mu\text{m}$ , purity:  $> 95\%$ ) used in this work are a commercial product supplied by Nanjing XFNANO Materials Tech Co., Ltd, China. The mixed cellulose ester (MCE) filter membrane is commercially available from Beijing Shenghe, China. The industrial oil-in-water nanoemulsion, which is a wastewater from a washing fractionating tower, was supplied by SINOPEC SABIC Tianjin Petrochemical Co., Ltd, China. All the other chemicals were of analytical grade and commercially available from Shanghai Chemical Reagent Co., Ltd.

### Fabrication of the SWCNT/PD dispersion

The SWCNT dispersion was prepared just as reported in our previous work.<sup>39</sup> In detail,  $0.1 \text{ mg mL}^{-1}$  SWCNT powder,

$1 \text{ mg mL}^{-1}$  sodium dodecyl benzene sulfonate and deionized water were mixed and sonicated for 10 h under a power of 2 kW. To obtain the SWCNT dispersion with a better dispersion degree, the as-prepared SWCNT dispersion was centrifuged for 30 min at 10 000 rpm. The supernatant solution was collected for the following experiments. The concentration of the prepared SWCNT dispersion was measured to be  $0.071 \text{ mg mL}^{-1}$ . Then the dispersion was diluted to be  $0.024 \text{ mg mL}^{-1}$ , and  $0.1 \text{ mg mL}^{-1}$  of dopamine was added into the dispersion. After stirring for 1 h, 10 mM HCl-Tris (pH = 7.5) was added into the dispersion and stirred for 36 h at  $40^\circ\text{C}$ . Then the dispersion was centrifuged at 10 000 rpm for 30 min and the supernatant solution was collected. The thickness of the PD layer on SWCNT was controlled by tuning the reaction time. The obtained PD-coated SWCNT (SWCNT/PD) dispersion (measured to be  $0.034 \text{ mg mL}^{-1}$ ) was kept at  $4^\circ\text{C}$  for further use.

### Fabrication of the SWCNT/PD/PEI composite film

The SWCNT/PD composite film was prepared through vacuum-filtering the SWCNT/PD dispersion onto a MCE filter membrane with a pore size of  $0.85 \mu\text{m}$ . The thickness and pore size of the obtained SWCNT/PD composite film was controlled by the amount of the SWCNT/PD dispersion filtered (see Fig. 3a for details). A SWCNT/PD composite film with a thickness of 154 nm, pore size of  $10 \pm 5$  nm, and effective filtration area of  $12.56 \text{ cm}^2$  could be obtained when 5 mL of the SWCNT/PD dispersion ( $0.034 \text{ mg mL}^{-1}$ ) was used. The SWCNT/PD film was then immersed in a water solution containing  $5 \text{ mg mL}^{-1}$  PEI (MW: 10 000) and 10 mM HCl-Tris (pH = 8.5) to graft PEI. After shaking slowly for 1 day at  $60^\circ\text{C}$ , the SWCNT/PD/PEI composite film was produced.

### Preparation of the oil-in-water nanoemulsions

The isooctane-in-water nanoemulsion was prepared by adding 5 mg of an isooctane–butanol solution (wt/wt = 1 : 1) into a 20 mL water solution containing 30 wt% Tween 80 and stirring the mixture to produce a yellowish solution. Then the solution was diluted 500 times to produce a transparent emulsion with a bluish tinge. The 1,2-dichloroethane-in-water nanoemulsion was prepared by adding 1 mL of 1,2-dichloroethane into a 100 mL water solution containing 0.3 wt% Tween 80 and stirring the mixture at a speed of 2000 rpm for 5 h to produce a transparent emulsion with a bluish tinge.

### Oil-in-water nanoemulsion separation

The separation process was carried out on a vacuum filter apparatus equipped with the SWCNT/PD/PEI composite film (support: MCE filter membrane, separation area:  $11.34 \text{ cm}^2$ ). 100 mL of the oil-in-water nanoemulsion was poured onto the film and the separation was achieved driven by a pressure difference of 0.5 bar. After separation, the filtrate water was collected.

## Characterization

The SEM images were measured on a field-emission scanning electron microscope (Hitachi S4800, Japan). The TEM images were measured on a Tecnai G2 F20 S-Twin field-emission transmission electron microscope. The water CA and underwater oil CA were measured on an OCA20 machine (Data-Physics, Germany). For each value, three measurements per sample were measured and the average value was obtained. The underwater oil adhesion force was measured using a high-sensitivity micro-electro-mechanical balance system (Data-Physics DCAT11, Germany). The oil content in the filtrate was detected on a total organic carbon (TOC) analyzer (Aurora 1030W, America). The dynamic light scattering was measured on a Malvern Zen 3600.

## Results and discussion

### Preparation and morphology characterization of the SWCNT/PD/PEI composite film

As schematically shown in Fig. 1a, the SWCNT dispersion is first produced and then a thin PD layer of several nanometers is coated onto the SWCNTs to obtain the SWCNT/PD dispersion. The SWCNT/PD dispersion is used to form the SWCNT/PD composite film through vacuum filtration of a certain amount of the SWCNT/PD dispersion onto a commercial MCE filter membrane. Then a PEI layer is grafted onto the SWCNT/PD composite film to produce the resulting SWCNT/PD/PEI composite film for nanoemulsion separation. Fig. 1b is an optical image of the free-standing and transparent SWCNT/PD/PEI composite film floating on the surface of an acetone–water mixture solution. The thickness of the SWCNT/PD/PEI composite film is 158 nm as confirmed by AFM measurement (Fig. 1c). Fig. 1d is a typical TEM image of the film with pores

(shown by dashed arrows) of several nanometers. The SWCNT/PD/PEI composite film shows a superhydrophilic and underwater superoleophobic wetting property. When a water droplet (3  $\mu$ L) is placed onto the film surface in air, it spreads completely within 3 s and a water contact angle (CA) of nearly zero is obtained (Fig. 1e). When an oil (1,2-dichloroethane is taken as an example) droplet is placed onto the film surface underwater, the oil droplet stays on the film without spreading with an oil CA of  $162^\circ$  (Fig. 1f).

Fig. 2 depicts the characterization of the PD-coated SWCNT with different coating time. The colour of the original SWCNT dispersion is charcoal grey. After coating with PD, the colour of the dispersion turns to brown (Fig. 2a). The TEM images clearly show the formation of the PD layer on the SWCNT surface. With an increase of the coating time from 2 h to 48 h, the thickness of

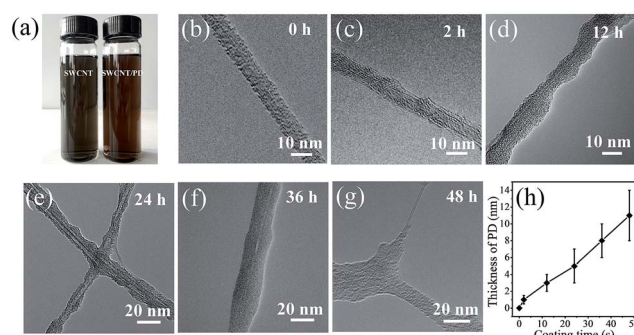


Fig. 2 (a) Digital photo of the SWCNT (left) and SWCNT/PD (right) dispersions. (b)–(g) TEM images of the PD-coated SWCNT with coating times of 0 h, 2 h, 12 h, 24 h, 36 h and 48 h. The corresponding thickness of the PD layer on SWCNT is 0 nm, 1–2 nm, 2–4 nm, 3–7 nm, 6–10 nm and 8–14 nm, respectively. (h) Statistical curve of the thickness of the PD layer on the SWCNT with increasing coating time.

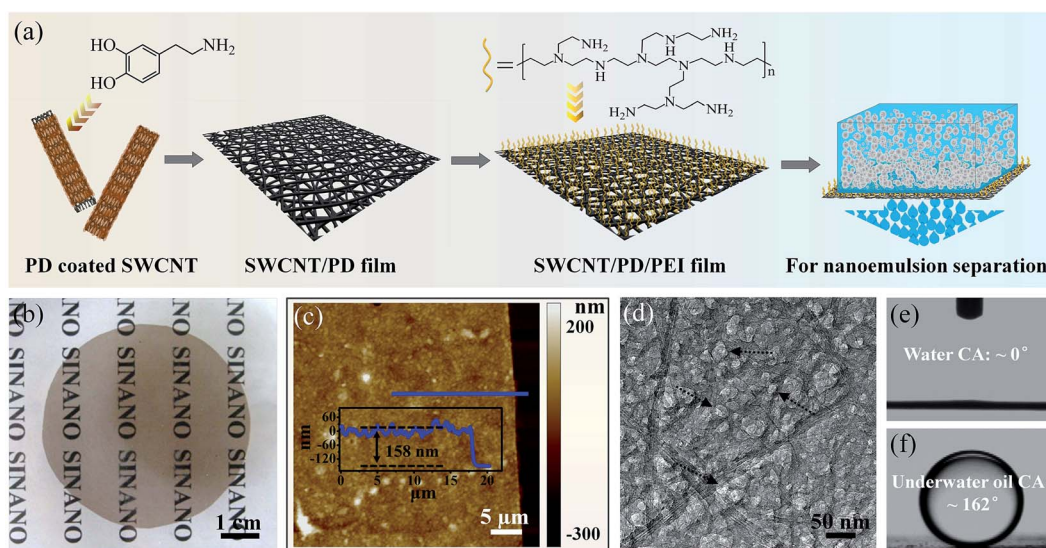


Fig. 1 (a) Preparation of the SWCNT/PD/PEI composite ultrathin film for the separation of an oil-in-water nanoemulsion. (b) Digital photo of a SWCNT/PD/PEI composite film floating on an acetone–water mixture solution. (c) AFM image and height profile of the SWCNT/PD/PEI composite film. (d) TEM image of the SWCNT/PD/PEI composite film. Photographs of a water droplet on the SWCNT/PD/PEI film in air (e) and an oil droplet on the film underwater (f).



the PD layer on the carbon nanotube increases gradually from 1–2 nm to 8–14 nm (Fig. 2b–g). Fig. 2h is a statistical curve showing the relationship between the PD layer thickness and coating time. It shows that the most uniform PD layer with a thickness of 3–7 nm on the SWCNT could be obtained when the coating time of PD on the SWCNT was 24 h. By prolonging the coating time, the thickness of the PD layer becomes thicker and not uniform, which will give rise to a SWCNT/PD composite film with a wide pore size and low mechanical stability, and aggregation and crosslinking among SWCNTs even form. In this work, the PD/SWCNT dispersion with the coating time of 24 h was used to form films and to graft PEI.

As for the SWCNT/PD composite film, its thickness is directly related to the pore size. By adjusting the amount of the SWCNT/PD dispersion to be filtered, the film thickness and the corresponding effective pore size of the film could be tuned. As shown in Fig. 3a and S1,<sup>†</sup> the pore size of the film decreases quickly with increasing the usage of SWCNT/PD. When the usage of SWCNT/PD is  $27 \text{ mg m}^{-2}$ , a SWCNT/PD composite film with a pore size of  $110 \pm 40 \text{ nm}$  could be obtained, while a SWCNT/PD composite film with a pore size as small as  $10 \pm 5 \text{ nm}$  could be obtained when the usage of SWCNT/PD was  $134 \text{ mg m}^{-2}$ . Correspondingly, the thickness of the film increases from 31 nm to 154 nm. The permeation flux of the SWCNT/PD composite film depends greatly on the film thickness and effective pore size. As shown in Fig. 3b, the pure water flux of the SWCNT/PD film decreases quickly with increasing film thickness from  $38\,800 \text{ L m}^{-2} \text{ h}^{-1} \text{ bar}^{-1}$  in the case of a 31 nm-thick film to  $8100 \text{ L m}^{-2} \text{ h}^{-1} \text{ bar}^{-1}$  in the case of a 154 nm-thick film. To separate oil-in-water nanoemulsions with oil droplets of tens of nanometers, a SWCNT/PD composite film with a pore size of  $10 \pm 5 \text{ nm}$  and thickness of 154 nm was chosen. To further confirm the effective pore size of the film,

nanoparticles including Au nanoparticles with a size of 8–14 nm (Fig. S2a<sup>†</sup>) and bovine serum albumin (BSA) with a size of 5 nm were filtered, respectively through the film and the rejection rates after filtration were measured by UV-vis spectroscopy. A rejection rate of 91% for Au nanoparticles was obtained (Fig. 3c) and a rejection rate of 40% for BSA was obtained (Fig. 3d). This reveals that the effective pore size of the 154 nm-thick SWCNT/PD film is in the range of 5–14 nm.

In order to improve the wetting property of the film, PEI (MW: 10 000) as a water-favoring polymer was grafted onto the film through a Michael addition or Schiff base reaction between PEI and PD, as has been widely confirmed by previous reports.<sup>47–49</sup> As shown in Fig. 4b and c, the film structure is almost unchanged after grafting PEI. The rejection rates of the SWCNT/PD/PEI composite film for the aforementioned Au nanoparticles and BSA are 93% and 51%, respectively, similar to those of the SWCNT/PD composite film. It indicates that the effective pore size of the SWCNT/PD/PEI composite film is almost the same as the SWCNT/PD composite film, and the grafting of PEI onto the SWCNT/PD film has no effect on the effective pore size. The pure water flux of the SWCNT/PD/PEI composite film is up to  $7270 \text{ L m}^{-2} \text{ h}^{-1} \text{ bar}^{-1}$ . To further confirm the grafting of PEI onto the SWCNT/PD film, C1s XPS spectra of the film were measured (below in Fig. 4a–c). As compared to the bare SWCNT film, the peak at 286.2 eV is observed for the SWCNT/PD composite film, which corresponds to C–O/C–N of PD. As for the SWCNT/PD/PEI composite film, a peak at 284.8 eV ascribed to  $-\text{CH}_2-$  is observed, suggesting the existence of the PEI layer.

### Wettability of the SWCNT/PD/PEI composite film

The surface wetting property of a membrane is crucial for high-efficiency oil–water separation. The pure SWCNT film has a hydrophobic property with a water contact angle (CA) of  $121^\circ$  and the water CA remains stable with time (Fig. 5a). Such a wetting property is not effective to separate oil-in-water emulsions. The SWCNT/PD composite film shows improved hydrophilicity with a water CA of  $72^\circ$  once the water droplet contacts the film surface and the water CA decreases slowly to  $45^\circ$  within 30 s. The SWCNT/PD/PEI composite film has a

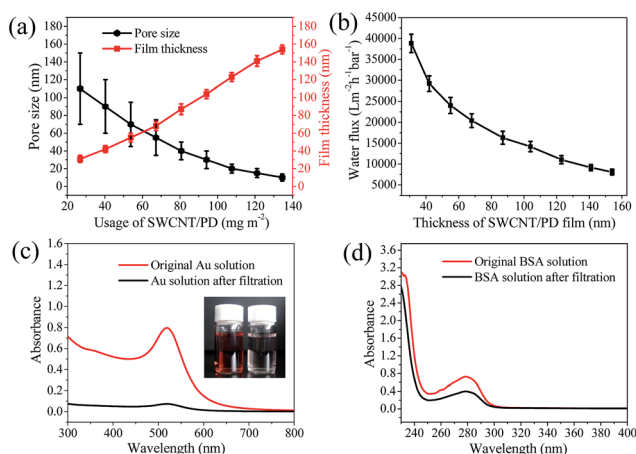


**Fig. 3** (a) Statistical curve of the pore size and thickness of the SWCNT/PD composite film with different usage of SWCNT/PD. (b) Variation of the pure water flux of the SWCNT/PD composite film as a function of film thickness. (c) UV-vis spectra of the Au nanoparticle solution before and after filtration by a 154 nm-thick SWCNT/PD composite film. The inset is a digital photo of the Au nanoparticle solution before (left) and after (right) filtration. (d) UV-vis spectra of the BSA solution before and after filtration by a 154 nm-thick SWCNT/PD film.

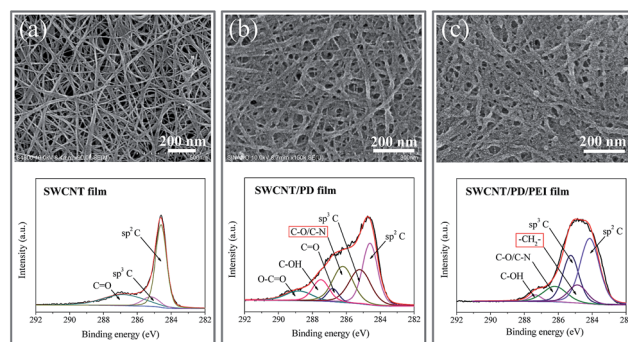


**Fig. 4** SEM images and corresponding C1s XPS spectra of the pure SWCNT film (a), the SWCNT/PD composite film (b), and the SWCNT/PD/PEI composite film (c).

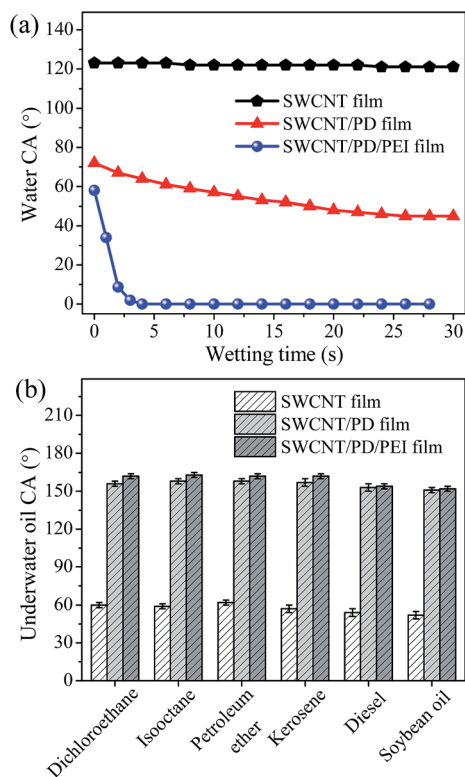


Fig. 5 Water CAs (a) and underwater oil CAs (b) of the pure SWCNT film, the SWCNT/PD composite film and the SWCNT/PD/PEI composite film.

superhydrophilic property with a final water CA of nearly zero and a water droplet can quickly permeate the film within 3 s. The underwater oil CAs of the three films were also measured as shown in Fig. 5b. For the six different oils, the pure SWCNT film shows an underwater oil CA of  $\sim 60^\circ$ . However, both the SWCNT/PD composite film and the SWCNT/PD/PEI composite film have an underwater superoleophobic property with underwater oil CAs all larger than  $150^\circ$ . These results indicate that the SWCNT/PD/PEI composite film has superior superhydrophilic and underwater superoleophobic properties, which are essential for oil–water separation. This is benefited from the PEI layer, which contains ample water-favoring amine groups. The SWCNT/PD/PEI composite film also exhibits an extremely low underwater oil adhesion force below  $1 \mu\text{N}$  (Fig. S3†). When a  $3 \mu\text{L}$  oil droplet (herein, 1,2-dichloroethane is taken as an example) is forced to sufficiently contact with the film surface and is then lifted up underwater, there is no force drop observed in the receding curve and the corresponding photographs of the oil droplet show nearly no deformation when the oil droplet leaves the film surface. These results confirm that the SWCNT/PD/PEI composite film has ultralow underwater oil adhesion, suggesting its excellent anti-oil-fouling property. Meanwhile, the ample amine groups in PEI could cross-link with PD to form a cross-linked network, which makes PD more stable even in alkaline conditions.

### Separation of oil-in-water nanoemulsions by the SWCNT/PD/PEI composite film

The superhydrophilic and underwater superoleophobic properties of the SWCNT/PD/PEI composite film endows its ability for oil–water separation. The SWCNT/PD/PEI composite film is flexible and robust enough to be transferred onto any kind of porous support for separation (Fig. S4†). Two surfactant-stabilized oil-in-water nanoemulsions (isooctane-in-water, 1,2-dichloroethane-in-water) and an industrial oil-in-water nanoemulsion (a production from SINOPEC SABIC TianJin Petrochemical Company Limited) with oil droplets of tens of nanometers were used to permeate through the SWCNT/PD/PEI composite film, respectively, to evaluate the separation performance of the film. The separation process was carried out *via* a dead-end flow mode under a 0.5 bar transmembrane pressure. All emulsions could be successfully separated by passing through the film once. As the oil droplet sizes in the emulsions are less than 100 nanometers, the emulsions are all transparent. Dynamic light scattering (DLS) measurements were used to test the oil droplet size distribution of the emulsions in the feeds and filtrates. As can be seen in Fig. 6a (left image), the isooctane-in-water nanoemulsion is transparent. When a 650 nm laser illuminates the emulsion from one side, a Tyndall effect is obviously observed, indicating the presence of oil droplets in the emulsion. The DLS curve shows that the oil droplet size of the emulsion feed is mainly distributed around 54 nm (right in Fig. 6a). After separation, no Tyndall effect could be observed in the filtrate, indicating that no oil droplets were left in the solution (left in Fig. 6b). The DLS curve also confirms the disappearance of oil droplets (right in Fig. 6b). It is worthy to note that the sharp peak appearing at 2 nm is caused by residual surfactants in the filtrate. Similar separation results were also obtained in the cases of the 1,2-dichloroethane-in-water nanoemulsion and the industrial nanoemulsion (Fig. S5†).

Fig. 7 summarizes the separation performance of the SWCNT/PD/PEI composite film for the three oil-in-water nanoemulsions. As shown in Fig. 7a, the oil droplet sizes of the three nanoemulsion feeds were mainly distributed in the range of 50–70 nm. However, no oil droplets around this range were observed after the separation. The oil contents in the filtrates

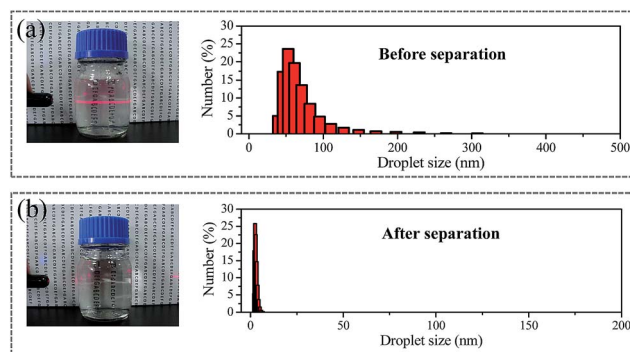


Fig. 6 Digital photo and DLS curve of the oil droplet size distribution of the isooctane-in-water nanoemulsion before (a) and after (b) separation by a SWCNT/PD/PEI composite film.

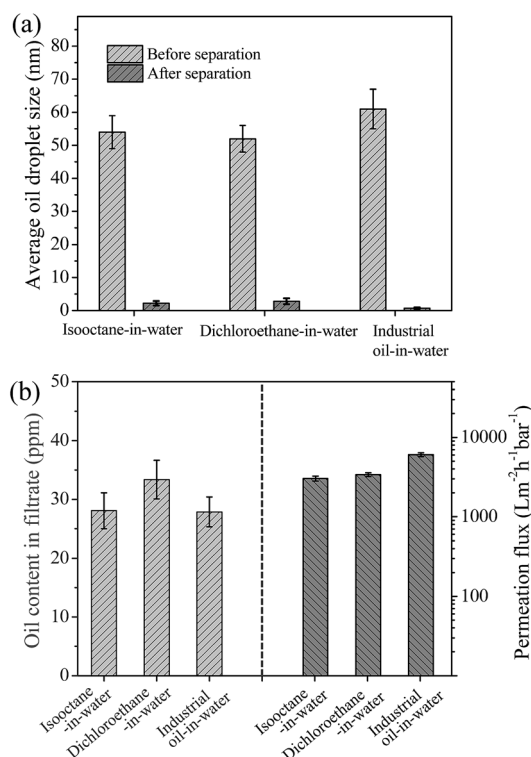


Fig. 7 (a) Droplet size distribution of the isooctane-in-water, dichloroethane-in-water and industrial oil-in-water nanoemulsions before and after separation by the SWCNT/PD/PEI composite film. (b) The oil contents in the filtrates (left) and permeation fluxes (right) of the isooctane-in-water, dichloroethane-in-water and industrial oil-in-water nanoemulsions separated by the SWCNT/PD/PEI composite film.

after the separation were measured *via* a TOC analyzer. It is worthy to note that the TOC value is the sum of both the oil and surfactant residues in the filtrate. The oil contents in the filtrates after a one-time separation were all below 35 ppm for the three emulsions (left in Fig. 7b). This value is lower than the discharge standards of the Environmental Protection Agency of the U.S. for offshore oil and gas activities and the discharge standard of the Ministry of Environmental Protection of China for wastewater from the off-shore petroleum development industry.<sup>50,51</sup> The SWCNT/PD/PEI nanocomposite film also exhibits extremely high separation fluxes for all three oil-in-water nanoemulsions of 3030 L m<sup>-2</sup> h<sup>-1</sup> bar<sup>-1</sup> for the isooctane-in-water nanoemulsion, 3390 L m<sup>-2</sup> h<sup>-1</sup> bar<sup>-1</sup> for the dichloroethane-in-water nanoemulsion, and 6060 L m<sup>-2</sup> h<sup>-1</sup> bar<sup>-1</sup> for the industrial oil-in-water nanoemulsion, respectively (right in Fig. 7b). These values are about 10 times higher than those of the traditional ultrafiltration membranes with similar rejection properties.<sup>10,11,17,18,52,53</sup> The flux differences between the different nanoemulsions are mainly ascribed to the different oil contents in the emulsion feeds (see Table S1†). Basically, an oil-in-water emulsion with a lower oil content exhibits a higher flux due to less oil fouling on the film. It is reasonably expected that the fouling issue could be depressed and the permeation flux could be further improved if the flow mode is changed from dead-end to cross flow.

### pH-stability and antifouling properties of the SWCNT/PD/PEI composite film

The pH-stability of the SWCNT/PD/PEI composite film is evaluated by monitoring the water CA and underwater oil CA of the film after the film is maintained in water solutions with a pH from 0 to 14 for more than 10 days. As shown in Fig. 8a, in the whole range of pH = 0–14, the SWCNT/PD/PEI film remains superhydrophilic and underwater superoleophobic. The excellent pH-resistance of the SWCNT/PD/PEI composite film indicates its potential for treating oil-containing wastewater in extreme pH conditions, which is superior to most of the polymer-based or ceramic-based membranes. It is worthy to note that the SWCNT/PD/PEI composite film is also very stable in common organic solvents such as ethanol and acetone.

Oil fouling is a common and tough issue for filtration membranes during the process of oil–water separation. An ideal membrane for oil–water separation should have a good antifouling property. The antifouling property of the SWCNT/PD/PEI composite film was monitored by detecting the change of permeation flux and separation efficiency during several cycles of nanoemulsion separation. For each cycle, 200 mL of the industrial nanoemulsion was permeated through the film and then the film was simply rinsed and soaked with a certain amount of 0.1 M HCl solution to remove the oils fouled on the film. The variation of the permeation flux during this process was tested. As shown in Fig. 8b, the permeation flux decreases

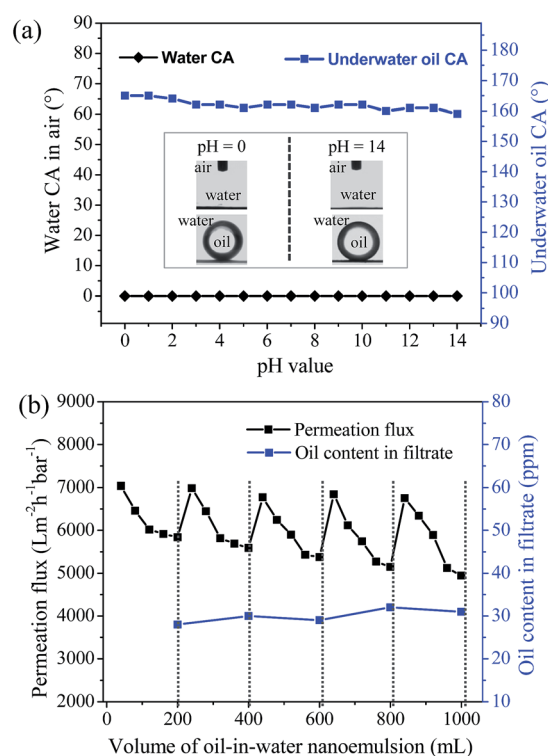


Fig. 8 Study of the pH-stability and antifouling property of the SWCNT/PD/PEI composite film. (a) Water CA and underwater oil CA of the film after the film was kept in water solutions with a pH from 0 to 14 for more than 10 days. (b) Real-time monitoring of the separation flux and oil content in the filtrate during the cycles of the antifouling test.



gradually with the increase of emulsion volume permeated through the film within one cycle and it can recover completely to the starting permeation flux after cleaning. The oil contents in the filtrate after separation were all below 32 ppm, indicating that the separation efficiency wasn't sacrificed during these cycles. These results demonstrate the excellent antifouling property of the SWCNT/PD/PEI composite film for the long-term use of treating oil-in-water nanoemulsions.

## Conclusions

Removing emulsified oils from wastewater has become a worldwide subject that is tough and challenging. Herein, SWCNT/PD/PEI composite ultrathin films which have super-hydrophilic and underwater superoleophobic properties were successfully prepared and used for the ultrafast separation of oil-in-water nanoemulsions with oil droplets of tens of nanometers in size. The ultrathin and robust SWCNT/PD/PEI composite film with a pore size of  $\sim 10$  nm and thickness of  $\sim 160$  nm can separate oil-in-water nanoemulsions with an ultrahigh permeation flux of up to  $6000 \text{ L m}^{-2} \text{ h}^{-1} \text{ bar}^{-1}$  with a high separation efficiency. Meanwhile, this film exhibits excellent pH-resistance and antifouling properties. This work points a direction for designing and fabricating ultrathin and super-wetting membranes to remove emulsified oils from wastewater, especially for oils at the nanometer scale. The SWCNT/PD/PEI ultrathin film has great potential for purifying emulsified wastewater from industries and daily life and for drinking water treatment.

## Acknowledgements

This work was supported by the National Basic Research Program of China (grant no. 2013CB933000), the National Natural Science Foundation of China (grant no. 21433012), the Key Development Project of Chinese Academy of Sciences (grant no. KJZD-EW-M01-3), and the Natural Science Foundation of Jiangsu Province (grant no. BK20130007).

## Notes and references

- 1 E. Kintisch, *Science*, 2010, **329**, 735–736.
- 2 J. Aurell and B. K. Gullett, *Environ. Sci. Technol.*, 2010, **44**, 9431–9437.
- 3 P. Kajitvichyanukul, Y.-T. Hung and L. K. Wang, in *Handbook of Environmental Engineering: Membrane and Desalination Technologies*, ed. Y.-T. Hung and L. K. Wang, The Humana Press Inc, New York, 2011, vol. 13, pp. 639–668.
- 4 M. A. Shannon, P. W. Bohn, M. Elimelech, J. G. Georgiadis, B. J. Mariñas and A. M. Mayes, *Nature*, 2008, **452**, 301–310.
- 5 T. Oki and S. Kanae, *Science*, 2006, **313**, 1068–1072.
- 6 J. Yeston, R. Coontz, J. Smith and C. Ash, *Science*, 2006, **25**, 1067.
- 7 H. Wang, K.-Y. Lin, B. Jing, G. Krylova, G. E. Sigmon, P. McGinn, Y. Zhu and C. Na, *Water Res.*, 2013, **47**, 4198–4205.
- 8 G. Kwon, A. K. Kota, Y. Li, A. Sohani, J. M. Mabry and A. Tuteja, *Adv. Mater.*, 2012, **24**, 3666–3671.
- 9 M. Chenyan and N. Rajagopalan, *J. Membr. Sci.*, 1998, **151**, 13–28.
- 10 M. M. Pendergast and E. M. V. Hoek, *Energy Environ. Sci.*, 2011, **4**, 1946–1971.
- 11 X. Wang, X. Chen, K. Yoon, D. Fang, B. S. Hsiao and B. Chu, *Environ. Sci. Technol.*, 2005, **39**, 7684–7691.
- 12 S. Maphutha, K. Moothi, M. Meyyappan and S. E. Iyuke, *Sci. Rep.*, 2013, **3**, 1509.
- 13 X. Chen, L. Hong, Y. Xu and Z. W. Ong, *ACS Appl. Mater. Interfaces*, 2012, **4**, 1909–1918.
- 14 Q. Chang, J. Zhou, Y. Wang, J. Liang, X. Zhang, S. Cerneaux, X. Wang, Z. Zhu and Y. Dong, *J. Membr. Sci.*, 2014, **456**, 128–133.
- 15 D. Rana and T. Matsuura, *Chem. Rev.*, 2010, **110**, 2448–2471.
- 16 L. Yang, A. Thongsukmak, K. K. Sirkar, K. B. Gross and G. Mordukhovich, *J. Membr. Sci.*, 2011, **378**, 138–148.
- 17 X. S. Yi, S. L. Yu, W. X. Shi, S. Wang, N. Sun, L. M. Jin and C. Ma, *Desalination*, 2013, **319**, 38–46.
- 18 I. Sadeghi, A. Aroujalian, A. Raisi, B. Dabir and M. Fathizadeh, *J. Membr. Sci.*, 2013, **430**, 24–36.
- 19 Y. Long, J. Hui, P. Wang, G. Xiang, B. Xu, S. Hu, W. Zhu, X. Lü, J. Zhuang and X. Wang, *Sci. Rep.*, 2012, **2**, 612.
- 20 J. Zimmermann, F. Reifler, G. Fortunato, L.-C. Gerhardt and S. Seeger, *Adv. Funct. Mater.*, 2008, **18**, 3662–3669.
- 21 J. Zhang and S. Seeger, *Adv. Funct. Mater.*, 2011, **21**, 4699–4704.
- 22 C. Gao, Z. Sun, K. Lin, Y. Chen, Y. Cao, S. Zhang and L. Feng, *Energy Environ. Sci.*, 2013, **6**, 1147–1151.
- 23 L. Zhang, Z. Zhang and P. Wang, *NPG Asia Mater.*, 2012, **4**, e8.
- 24 L. Zhang, Y. Zhong, D. Cha and P. Wang, *Sci. Rep.*, 2013, **3**, 2326.
- 25 Q. Zhu and Q. Pan, *ACS Nano*, 2014, **8**, 1402–1409.
- 26 N. Chen and Q. Pan, *ACS Nano*, 2013, **7**, 6875–6883.
- 27 F. Zhang, W. Zhang, Z. Shi, D. Wang and J. Jin, *Adv. Mater.*, 2013, **25**, 4192–4198.
- 28 Z.-Y. Wu, C. Li, H.-W. Liang, Y.-N. Zhang, X. Wang, J.-F. Chen and S.-H. Yu, *Sci. Rep.*, 2014, **4**, 4079.
- 29 J. Ge, Y.-D. Ye, H.-B. Yao, X. Zhu, X. Wang, L. Wu, J.-L. Wang, H. Ding, Y. Ni, L.-H. He and S.-H. Yu, *Angew. Chem., Int. Ed.*, 2014, **53**, 3612–3616.
- 30 J. Wang, K. Ren, H. Chang, S. Zhang, L. Jin and J. Ji, *Phys. Chem. Chem. Phys.*, 2014, **16**, 2936–2943.
- 31 Y. Cao, X. Zhang, L. Tao, K. Li, Z. Xue, L. Feng and Y. Wei, *ACS Appl. Mater. Interfaces*, 2013, **5**, 4438–4442.
- 32 A. K. Kota, G. Kwon, W. Choi, J. M. Mabry and A. Tuteja, *Nat. Commun.*, 2012, **3**, 1025.
- 33 A. K. Kota, Y. Li, J. M. Mabry and A. Tuteja, *Adv. Mater.*, 2012, **24**, 5838–5843.
- 34 W. Zhang, Z. Shi, F. Zhang, X. Liu, J. Jin and L. Jiang, *Adv. Mater.*, 2013, **25**, 2071–2076.
- 35 Z. Xue, S. Wang, L. Lin, L. Chen, M. Liu, L. Feng and L. Jiang, *Adv. Mater.*, 2011, **23**, 4270–4273.
- 36 X. Gao, L.-P. Xu, Z. Xue, L. Feng, J. Peng, Y. Wen, S. Wang and X. Zhang, *Adv. Mater.*, 2014, **26**, 1771–1775.

- 37 M. Tao, L. Xue, F. Liu and L. Jiang, *Adv. Mater.*, 2014, **26**, 2943–2948.
- 38 P. Cheng and Z. Xu, *Sci. Rep.*, 2013, **3**, 2776.
- 39 S. J. Gao, Z. Shi, W. Zhang, F. Zhang and J. Jin, *ACS Nano*, 2014, **8**, 6344–6352.
- 40 T. G. Mason, J. N. Wilking, K. Meleson, C. B. Chang and S. M. Graves, *J. Phys.: Condens. Matter*, 2006, **18**, R635–R666.
- 41 H. D. Silva, M. Â. Cerqueira and A. A. Vicente, *Food Bioprocess Technol.*, 2012, **5**, 854–867.
- 42 L. Wang, X. Li, G. Zhang, J. Dong and J. Eastoe, *J. Colloid Interface Sci.*, 2007, **314**, 230–235.
- 43 C. Lovelyn and A. A. Attama, *J. Biomater. Nanobiotechnol.*, 2011, **2**, 626–639.
- 44 S. B. Bernardi, T. A. Pereira, N. R. Maciel, J. Bortoloto, G. S. Viera, G. C. Oliveira and P. A. Rocha-Filho, *J. Nanobiotechnol.*, 2011, **9**, 44.
- 45 X. S. Peng, J. Jin, Y. Nakamura, T. Ohno and I. Ichinose, *Nat. Nanotechnol.*, 2009, **4**, 353–357.
- 46 C. C. Striemer, T. R. Gaborski, J. L. McGrath and P. M. Fauchet, *Nature*, 2007, **445**, 749–753.
- 47 H. Lee, S. M. Dellatore, W. M. Miller and P. B. Messersmith, *Science*, 2007, **318**, 426–430.
- 48 D. Schaubroeck, Y. Vercammen, L. V. Vaeck, E. Vanderleyden, P. Dubrueel and J. Vanfleteren, *Appl. Surf. Sci.*, 2014, **303**, 465–472.
- 49 M. Li, J. Xu, C.-Y. Chang, C. Feng, L. Zhang, Y. Tang and C. Gao, *J. Membr. Sci.*, 2014, **459**, 62–71.
- 50 GEG460000 for “Offshore Oil and Gas Activities in the Eastern Gulf of Mexico” by the Environmental Protection Agency, Washington, U.S., 2009.
- 51 GB 4914-85 for “Effluent Standards for Oil-Bearing Waste Water from Off Shore Petroleum Development Industry” by the Ministry of Environmental Protection, China, 1985.
- 52 X. Zhu, W. Tu, K.-T. Wee and R. Bai, *J. Membr. Sci.*, 2014, **466**, 36–44.
- 53 P. H. H. Duong and T.-S. Chung, *J. Membr. Sci.*, 2014, **452**, 117–126.